JOURNAL OF MATERIALS SCIENCE **37** (2002) 1599–1609

Characterisation of crosslinked polyethylene materials by luminescence techniques

G. TEYSSÈDRE*, G. TARDIEU, C. LAURENT
Laboratoire de Génie Electrique, Université Paul Sabatier, 118 route de Narbonne, 31062 Toulouse, France
E-mail: teyssedr@lget.ups-tlse.fr

Luminescence features of cross-linked polyethylene samples peeled from high voltage cables have been investigated. Special emphasis is given to the effect of crosslinking by-products on the emission. Photoluminescence and luminescence following excitation by a silent discharge have been examined in order to identify which of the luminescent centres are optically active following electrical charge recombination, and could therefore act as charge traps. Both fluorescence and phosphorescence contain signatures of volatile and bound species. However, the identification of the origin of these emissions is far from complete. The signature of acetophenone has been clearly identified in the phosphorescence spectra. Radiative charge recombination involves the long lived components of the phosphorescence spectrum, i.e. the lowest lying triplet states. Some routes are given for identifying more precisely the origin of the emissions.

1. Introduction

Crosslinked Polyethylene (XLPE) is increasingly used as insulation in AC high voltage buried power transmission cables, i.e. rated above 60 kV. The major advantages of XLPE over the competitive technology based on traditional oil-impregnated paper insulation are lower dielectric losses, less complicated installation procedure and maintenance, and no risk of leakage implying improved respect for environment. The technical limitations of XLPE-insulated high voltage cables are related to a lack of knowledge of the degradation withstanding ability of the insulation. The aim of the European project named ARTEMIS [1] is to investigate degradation processes and derive diagnostic properties for ageing evaluation and modelling of high-voltage XLPE cables. For this purpose, high voltage AC cables were produced using extra-clean materials and processes. The project started with the initial characterisation of cable insulation, in order to constitute the reference for electrical, micro-structural, and chemical properties needed to single out ageing markers on the basis of the property evolution with ageing time. The model which is being developed attempts to evaluate the role of trapped space charge on the ageing mechanisms of the insulation. Luminescence measurements were introduced as part of the characterisation tools. Depending on the excitation means, luminescence features may provide information related to chemicals, or to the interaction between electrical charges and groups acting as deep traps. These techniques can therefore be considered as at the frontier between physico-chemical and electrical characterisation tools. Three kinds of measurements are currently undertaken :

(i) Photoluminescence which provides a fingerprint of luminescent species which are initially present in the insulation. Both extrinsic (additives, crosslinking by-products) and intrinsic (oxidised groups, insaturations) chromophores are potentially emitting groups in XLPE materials.

(ii) Recombination induced luminescence which aims at identifying chromophores which are electrically active, i.e. which act as trapping centres. Charges of both polarities are implanted in the sample by a silent discharge and the light emitted upon dissipation of these charges is analysed.

(iii) Electroluminescence which refers to light emitted intrinsically by the material under field (excluding gaseous discharges). Only two mechanisms of light generation can be envisaged: (i) the recombination of charges of opposite polarities in the same region, and (ii) hot carrier processes (impact excitation or ionisation).

In electroluminescence, emission may arise from already-present species relaxing through a physical pathway, or from species produced in the excited state in the final step of a reaction [2]. As it is difficult to deduce which pathway is effective from the analysis of the electroluminescence spectrum alone, the information from the other two techniques is of prime importance. The present paper summarises our current

* Author to whom all correspondence should be addressed.

advancement in the characterisation of reference cable materials by photoluminescence and recombination-induced luminescence. A major challenge in this kind of study on complex materials is the identification of the nature of the emitting groups. Indeed, in a conventional dicumyl-peroxide cross-linked polyethylene formulation, numerous candidates as emitting centres can be envisaged, e.g. acetophenone, cumyl alcohol, α-methylstyrene, cumene, . . . , as crosslinking by-products, and antioxidants. In cables, low molecular weight species diffusing from the semiconducting screens into the insulation are also possibly emitting. This paper gives an overview of the luminescence features in this kind of material and proposes some route for identifying luminescent centres.

2. Materials

2.1. Cables reference

Two high voltage cables insulated by XLPE were produced specially for the Artemis project. The insulation thickness was 14 mm. Samples cut from the insulation of these cables are referenced A and B. Another cable with 27 mm-thick XLPE insulation has been introduced in the project for validating the present approach, since it was available in both the unaged and aged forms. Samples from this reference cable are labelled C. For the purpose of this paper, consideration of several unaged materials is made with the aim to generalise the kind of response obtained in XLPE cable insulation, and not to systematically compare these materials.

2.2. Samples handling

In this project, most of the basic characterisation of the materials can be carried out only on films. Therefore, measurements were performed on samples cut from the cables, having width 80 mm and mean thickness 150 μm. In order to minimise effects of diffusion of low molecular weight species from the screen, samples corresponding to the region 2 to 4 mm from the inner screen of the cable were analysed. More details on the effect of sample handling and cutting procedures on the measurements are given elsewhere [3]. A further problem that was considered is the preconditioning of the specimens before any measurement, in order to have reproducible results. It is clear that not all cross-linking by-products will exit the cable during ageing and thus could contribute to degradation processes. On the other hand, it is necessary to prepare samples whose properties change little with storage time. Therefore, a preconditioning procedure in which the samples were placed in an oven for 48 h at 50°C in order to expel cross-linking by-products has been adopted. No by-products were detected after such treatment using either HPLC or FTIR [3, 4]. As the luminescence features of these by-products are of interest, we have compared results obtained on specimens before and after preconditioning.

3. Techniques

3.1. Set-up

The experimental set-up is designed in such a way that low level light emission from polymers may be measured in-situ for various kinds of excitation, being either electrical field [5], cold plasma [6], UV, or temperature (for chemiluminescence, see e.g. ref. 7). A regulation system allows to set temperature in the range [-180, $+180$°C] with an accuracy of 2°C at atmospheric pressure. A pumping unit produces pressures of order 10^{-7} mbar. The chamber is equipped with electrical feedthroughs for high voltage input and temperature or current measurement. The light-tight chamber is organised around three optical axes equipped with windows and lenses made of quartz. These axis are used for UV-excitation, integral light detection, and spectral resolution. Integral light detection is made using a cooled photomultiplier (PM) working in photon counting mode with Ortec counting electronics. The spectral analysis of the emitted light is made using a grating monochromator coupled to a liquid nitrogen cooled CCD camera. The analysis range is 220–840 nm and the resolution is 4.5 nm in the configuration used. For both integral and wavelength resolved detection, the light is collected along a direction perpendicular to the plane of the sample film. A schematics of the set-up can be found in reference [7].

3.2. Photoluminescence (PL)

Luminescence emitted by the samples upon UV-excitation was analysed. It provided a signature of luminescent centres in the samples. Room temperature and liquid nitrogen temperature experiments allowed characterization of the fluorescence and phosphorescence respectively of the material. Experiments were performed with gaseous helium at atmospheric pressure as thermal exchange gas. UV excitation was made in the range 220–300 nm by means of a Xenon lamp coupled to a double-pass irradiation monochromator. The bandwidth of excitation was about 2 nm and emission spectra were acquired with the CCD. Phosphorescence lifetime measurements were realised using the excitation shutter closure as trigger for the PM counting system. A wide bandwidth ($\approx$40 nm) filter centred at the phosphorescence emission peak (450 nm) was inserted on the optical path to remove unexpected components of the light (fluorescence and excitation beam). Special emphasis will be given to the signature of strongly versus weakly bounded luminescent species by considering the effect of sample pre-conditioning.

3.3. Recombination-induced luminescence

This procedure gives access to the signature of the species specifically involved in charge recombination. Charges of both polarities were deposited on one surface of the sample during exposure to a silent discharge produced in helium at atmospheric pressure between two parallel electrodes. The sample was deposited on the lower one and the upper one was a transparent indium-tin oxide (ITO) film laid on a quartz disk in such a way that the discharge was initiated between two dielectrics, namely the upper surface of the sample and the quartz disk. The plasma gap of 5 mm was powered at a frequency of 5.5 kHz under a voltage of about 1.5 kV r.m.s. Before introducing the helium, the chamber was pumped down

to 10^{-5} mbar. Experiments were undertaken at liquid nitrogen temperature to enhance emission, and using short interaction time (5 s) to ensure negligible surface transformation. The decay of light emitted by the sample after discharge switch off was analysed in both the integral and wavelength-resolved forms. At short time, luminescence excited through processes other than radiative recombination was detected. The analysis of the decay kinetics of the integral light allowed an unambiguous determination of the time range where recombination was the dominant excitation mechanism. The related emission spectrum was identified accordingly. We refer to PIL (plasma-induced luminescence) for the global information, irrespective of the excitation mechanism, and to RIL (recombination-induced luminescence) for the part of the signal related to electrical charge recombination. Once isothermal luminescence measurements were completed, thermoluminescence was recorded while heating the sample at a constant rate of 5°C/min form –180°C up to 30°C. Thermal detrapping of charges is expected to occur at the relaxation temperatures of the material, giving rise to enhanced emission. Again, the influence of pre-conditioning on the response was investigated.

4. Results

4.1. Photoluminescence

4.1.1. Fluorescence

Fluorescence in these materials is very complex as several close-lying bands are detected and superposed to a large extent, irrespective of the excitation wavelength.

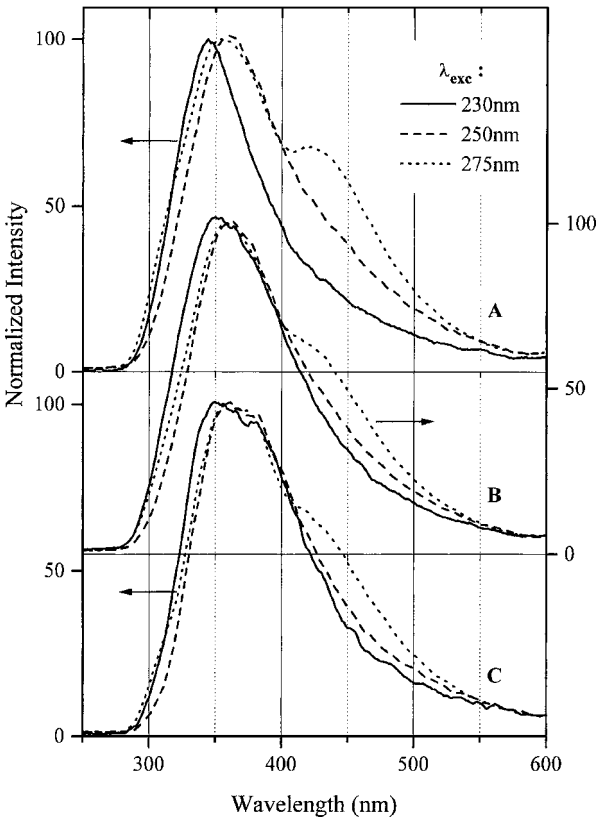

Figure 1 Room temperature photoluminescence emission spectra of preconditioned peelings from cables A, B and C for different excitation wavelengths. Spectra were normalized to their maximum intensity ($I_{max} = 100$).

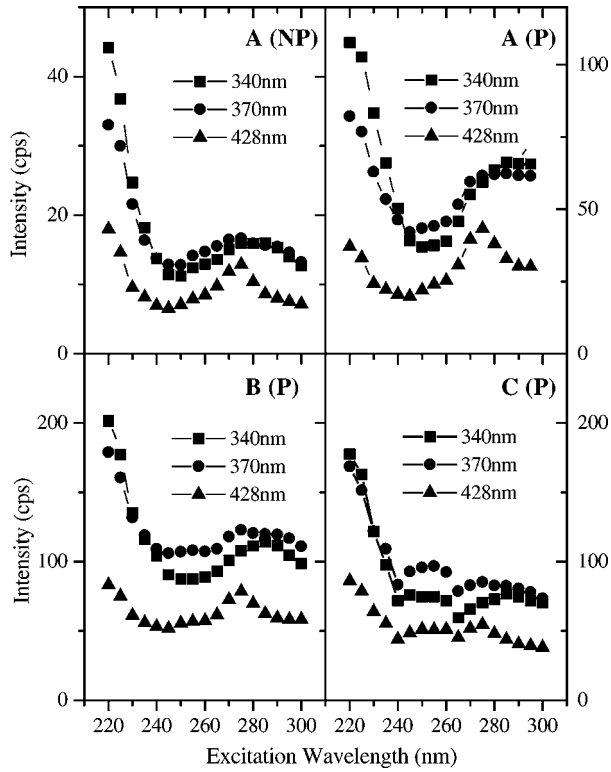

Figure 2 Room temperature photoluminescence excitation spectra of as-received (NP) and preconditioned (P) cable A (top), and preconditioned cables B and C (bottom) monitored at the emission wavelengths indicated in the legend.

Fig. 1 shows the principal features of the emission spectra obtained from preconditioned samples. Fig. 2 shows the corresponding excitation spectra monitored at the peak wavelength of the components identified in the emission spectra. The excitation spectra have been corrected for the wavelength dependence of the excitation power. However, the region 220–230 nm is probably overestimated. Therefore, these spectra should be considered only for comparison of the relative emission yield of the different materials. The effect of preconditioning is shown on the excitation spectra for cable A, which is known as the material containing the highest content of volatile species, due to extrusion conditions. At least 3 emission bands have been identified:

- an emission at 340 nm, which is best resolved when exciting at short wavelength (230 nm, see Fig. 1). The relative intensity of this band is weaker in samples B and C which contain less volatile species. Therefore, it might be characteristic of volatile groups. However, we did not detect any clear effect of preconditioning on the strength of the band.
- an emission in the range 360–375 nm, with excitation band at about 280–290 nm. Preconditioning strengthens this band. As emissions peaking at 340 and 360–375 nm are close-lying and relatively broad, the related excitation spectra cannot be easily distinguished. In sample C, a component at around 380 nm appears distinctly (see Fig. 1). It is also detected as a shoulder for the other two cables, specially for the spectrum under excitation at 250 nm. Considering the excitation spectra, this component corresponds to a peak at 250 nm in the excitation spectrum of sample C which is not seen

for the other samples. The growing of this band is possibly in relation to the fact that cable C was stored for a long time after cable production.

– an emission at around 425 nm with excitation peak at 275 nm. This emission has been obtained so far only in cross-linked polyethylenes, including materials produced in film form. This feature excludes the possibility of luminescence arising from species diffusing from semiconducting screens as may happen in cables. The fluorescence of low density polyethylenes is comparatively more simple with a main emission at around 335 nm [8]. Hence, this emission is clearly a characteristic of crosslinked polyethylenes. It seems not to be related to volatile species since preconditioning enhances it.

In case of material A, the emission is strengthened by a factor of about 3 after preconditioning. We observed that it still increased in a sample previously treated at 50°C for 2 days and kept at this temperature for one extra day. One would expect a decrease of the emission rather than an increase since volatile products, which are candidate as emitters, are removed at higher temperature. However, the increase of the emission does not necessarily mean that more emitting species are produced. It could result from removal of either strongly absorbing species which do not emit and/or from efficient quenching (energy transfer) of the excitation of the emitting groups by non-emitting species. In the first situation, one would expect a different UV-vis transmission spectrum after thermal treatment. In the second case, the change of shape of the excitation spectrum would be indicative of different quenching efficiency and/or difference in the volatility of emitting species. In any case fluorescence measurements can be indicative of the quantity of remaining by-products.

4.1.2. Phosphorescence

In photoluminescence experiments undertaken at −185°C, i.e. close to liquid nitrogen temperature, a much stronger emission is obtained. This emission is red-shifted with respect to the fluorescence of the material, and is referred to as phosphorescence. Fluorescence corresponds to allowed transitions between a singlet excited state and ground state; the related lifetime is extremely short (order of ns). Conversely, phosphorescence corresponds to a triplet to singlet transition, and is spin-forbidden. As the corresponding lifetime is much longer (ms to s), triplet excited states are very likely to transfer their energy to their surroundings, and so the emission is quenched. Molecular oxygen is known as a very efficient quencher [9]. Lowering the temperature freezes molecular groups in a certain configuration and reduces the probability of interaction with surrounding groups. Since the diffusion of molecular oxygen is affected by relaxation processes involving local molecular motion, the temperature dependence of phosphorescence should also reflect relaxation phenomena.

The emission spectra obtained at –185°C are shown in Fig. 3. Results for as-received and preconditioned sample A are compared. These spectra are representative of what was obtained on the other materials. The excitation spectra (not shown) exhibit two maxima, at about 240–250 nm and 280 nm for all the samples. They differ markedly from the excitation spectrum of fluorescence, which means that phosphorescing species are different from fluorescing species. A strongly structured emission, significantly dependent on the excitation wavelength, was obtained for the as-received material. This structure is best resolved when exciting at 240 nm. Several maxima are found at 388, 415, 443, 476, and 515 nm. These results show that at least two kinds of species contribute to the phosphorescence emission. They have distinct excitation spectra with maxima estimated at around 240 nm and 280 nm.

As for fluorescence (see Fig. 2), preconditioning of sample A increased the emission by a factor ≈2. After preconditioning, the spectrum did not evolve greatly when changing the excitation wavelength. Upon excitation at 240 nm, the structure described above was also

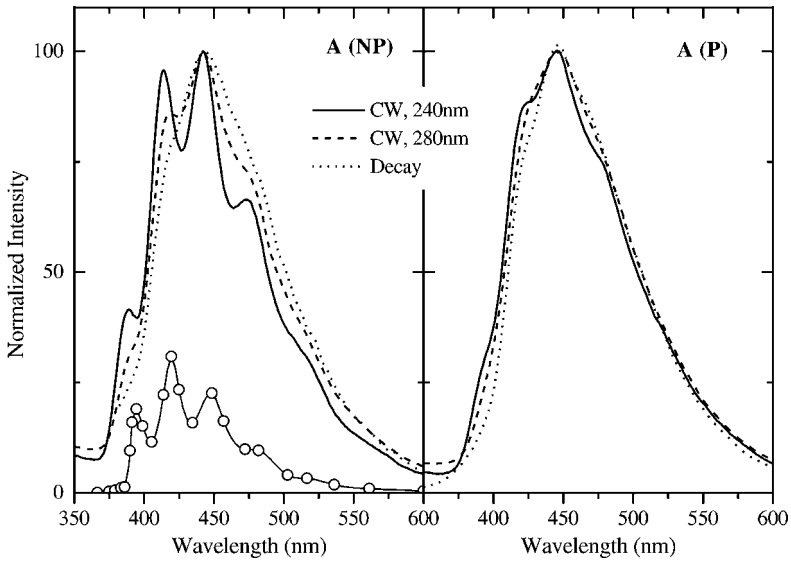

Figure 3 Phosphorescence spectra obtained at liquid nitrogen temperature on as-received (NP) and preconditioned (P) sample A. The spectra during the decay were obtained with an integration time of 1 s. Circles indicate the phosphorescence spectrum of acetophenone [9]. CW = continuous wave excitation.

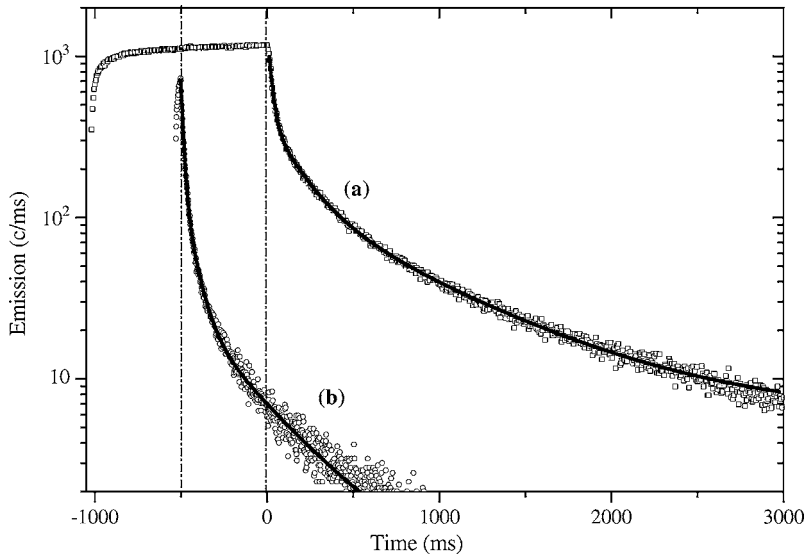

Figure 4 Phosphorescence decay obtained using excitation duration of 1 s (a) and 1/30 s (b). The counting dwell times were 5 ms and 2 ms, respectively. Lines are fits to a sum of 3 exponential decays.

detected. The spectrum obtained along the phosphorescence decay is also represented on Fig. 3.

Our present understanding of these phosphorescence spectra is that at least two kinds of species contribute to the emission: acetophenone and an unspecified one. There is no doubt that the structured emission is related to acetophenone. The position in wavelength of the bands is in good agreement with literature data as shown in Fig. 3 [10]. The spectrum shown as circles was obtained at 80 K in solid solution of EPA (ether, isopentane and ethanol mixture). The structured emission is due to the relaxation of triplet states involving ground state vibrations of the chromophore. The vibronic structure of acetophenone phosphorescence emission was perfectly resolved at 4 K, and the strongest bands have been identified as harmonics of the ν (C=O) Raman band at 1684 cm^{-1} [11]. At 80 K, the energy difference between the bands shown in Fig. 3 is about 1530 cm^{-1} (0.19 eV), for both acetophenone and sample A. This change in the vibration energy is possibly due to overlapping of several vibronic states. The point is that the bands are equally spaced in energy, which implies that the main structure arises from the same excited state of acetophenone.

Further evidence of the involvement of acetophenone is provided by the phosphorescence decay measurements shown in Fig. 4. Two decays have been recorded using different excitation times. Acquisition was averaged over several decays to improve the signal-to-noise ratio. The kinetics governing emission build-up at excitation switch-on are normally the same as during the decay [12]. In case of chromophores with distributed lifetimes, short-lived species can in principle be excited selectively by using appropriate excitation time. This rule is verified here since the decay is faster for the shorter excitation time (1/30 s). With an excitation time of 1 s, the steady state phosphorescence level was not reached. It is still increasing just before switch off at a rate of around 8%/s. Therefore, a slower decay would probably be obtained using a longer excitation time. These decays have been analysed as the sum of 3 exponential functions and the obtained results are listed in Table I. Note that there is no physical reason to consider the decay as a sum of 3 or more processes other than to give a rough estimation of the time scale of the phenomena. However, this analysis confirms the fact that several species contribute to the emission as deduced from a comparison of the CW and decay spectra (Fig. 3). The fastest process has a radiative lifetime of no more than 15 ms. This result is in agreement with previous reports on the phosphorescence lifetimes of acetophenone [11, 13]. The prominent structure and the short lifetime are strong indications that acetophenone phosphorescence corresponds to the relaxation of an n-π^* state.

TABLE I Parameters of the fit of phosphorescence decay as the sum of 3 exponential decays with A_i as pre-exponential factors and τ_i as lifetimes

Exc. Time (s)	A_1 (c/ms)	τ_1 (ms)	A_2 (c/ms)	τ_2 (ms)	A_3 (c/ms)	τ_3 (ms)
1	5167	23.4	1426	171	632	745
1/30	4859	14.5	1369	62	252	366

Neither the shape of the spectrum obtained during the decay, nor the slow components of signal decay, can be accounted for by acetophenone alone. We have recorded several time-resolved spectra during the decay. No change in the shape of this spectrum was observed at times more than about 0.5 s after excitation cut-off, whatever the sample. This behaviour means that these decay spectra are characteristic of long-lived excited states other than the n-π^* states of acetophenone. From the analysis of the decay (either from spectrum magnitude vs. time, or integral light decay) it can be inferred that the lifetime of these species is in the range 0.5–1.5 s.

Fig. 5 compares the phosphorescence decay spectra obtained in the time range 0.5–6 s after excitation switch-off. The shape of the spectrum varies from one sample to another. In case of sample A, a structure resembling that of acetophenone appears. In case of sample B, the spectrum is broader than for sample A

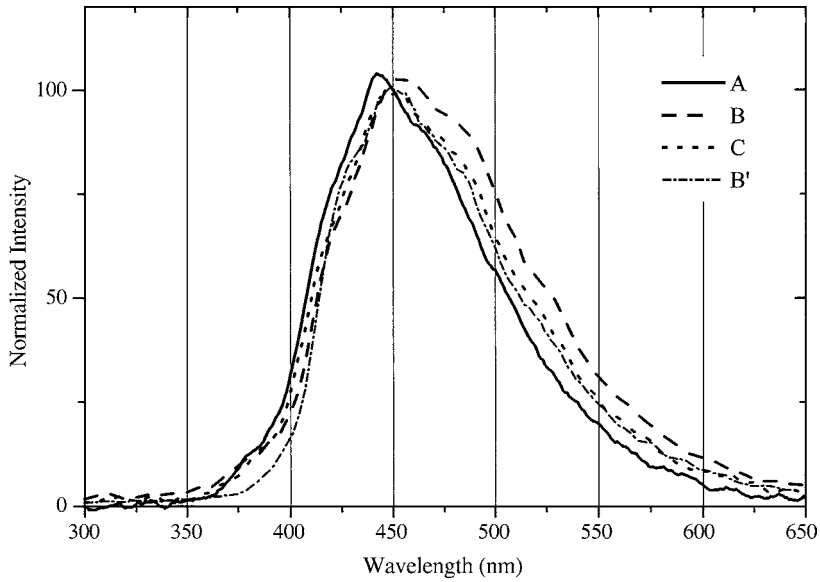

Figure 5 Phosphorescence decay spectra obtained in preconditioned samples A, B and C in the time range 0.5–6 s after excitation switch-off. Spectrum B′ refers to decay for sample B in the time range 0–0.1 s.

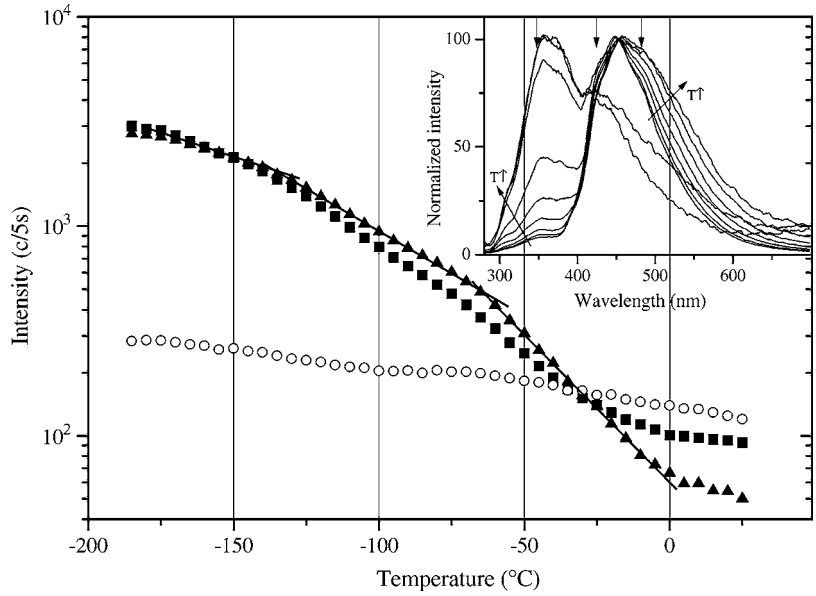

Figure 6 Temperature dependence of photoluminescence monitored at different emission wavelengths in preconditioned sample B. $\lambda_{exc} = 275$ nm. Squares: phosphorescence at 425 nm; Triangles: phosphorescence at 482 nm; Circles: fluorescence at 350 nm. In inset: normalized spectra taken at 25°C intervals from −185 to +15°C.

(width at mid-height of 115 nm compared to 95 nm for sample A) and the maximum is red-shifted. The decay spectrum obtained within 0.1 s after excitation switch-off is also represented in this figure. Emission in the long wavelength range is lower than in the spectrum in the interval 0.5–6 s and the spectrum resembles the one of sample C. This behaviour apparently results from the contribution of another structured emission with bands at approximately 10 nm higher than in acetophenone. The lifetime of this extra-contribution is relatively long (some seconds). Hence, at least 3 contributing species appear active in phosphorescence, and their relative magnitude changes from sample to sample.

The temperature dependence of photoluminescence has been recorded while heating the samples at 5°C/min. Spectra were recorded in steps of 5°C, and the evolution of the emission at specific bands is shown in Fig. 6 along with several spectra in 25°C intervals. The phosphorescence decreases by nearly 2 orders of magnitude over the whole temperature range. Similar results were obtained irrespective of the material and of previous preconditioning. The phosphorescence spectrum broadens in its long wavelength part as the temperature is raised. From −60°C and on, fluorescence at 430 nm becomes important and the intensity at 425 nm is a superposition of fluorescence and phosphorescence. However, the intensity at 482 nm is still decreasing. The decrease of the emission lets appear two transition regions at about −135°C and −60°C as defined by the intersection of the lines drawn. They have a possible relation with the secondary γ- and β-relaxations of the material. This behaviour will be further discussed in relation to the thermoluminescence curves.

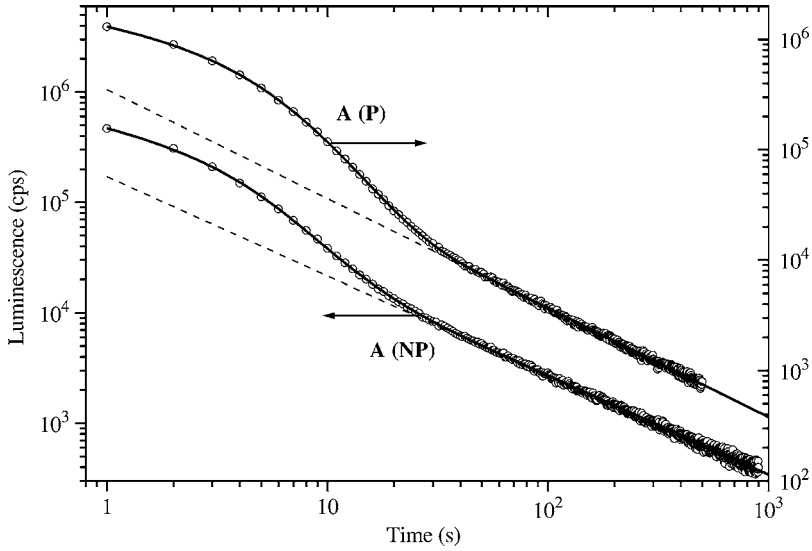

Figure 7 Isothermal luminescence decay at −185°C following excitation of sample A by a silent discharge and fit to equation I (solid line). The dashed line represents the contribution of RIL.

4.2. Recombination-induced luminescence (RIL)

4.2.1. Integral light decay

Fig. 7 shows a typical example of integral light decay following excitation of the surface of the film by a silent discharge for about 5 s. Light could be measured for more than 15 min after excitation switch-off: such long-lived decay is not consistent with the lifetime of excited states, and thus other excitation mechanisms, such as the kinetics of charge recombination, control this decay. At long time, this decay follows approximately an hyperbolic law in time (t^{-m}).

This form of decay can be explained by a tunnelling-mediated charge recombination mechanism involving a homogeneous distribution of electron-cation distances [14, 15], confirming hence that the signal is characteristic of charge recombination. Actually, an alternative explanation of such decay law is thermal detrapping assuming an appropriate distribution of trap depth and first order kinetics, as reviewed in [16]. The tunnelling mechanism is preferred to thermal detrapping because the decay kinetics are essentially temperature independent when experiments are undertaken at 80 K or 300 K [8], which is not expected in case of thermal detrapping.

The other contribution appearing at short time is due partly to the decay of phosphorescence induced by the UV of the discharge. In order to account for the decay in the whole time range of measurement, the following equation has been used for fitting :

$$I = I_1 \cdot \exp\frac{-t}{\tau_1} + I_2 \cdot \exp\frac{-t}{\tau_2} + I_3 \cdot t^{-m} \qquad (1)$$

The exponential decays describe the short time range of the signal whereas the power law represents the part due to radiative charge recombination. As acquisition was run about 1 s after excitation switch-off, processes having lifetimes in the ms range were not detected with this procedure. The use of two exponential decays, with time constants in the range of seconds, was necessary to give a good description of the total light decay. The parameters of the fits are listed in Table II for the different materials that have been tested. As the emission yield can not be easily compared from one sample to another, due to experimental conditions, the preexponential factors have been normalised to I_3. The last column represents the time above which the contribution of the power law to the total signal exceeds 90%. RIL is the dominant emission mechanism after about 30 s in the decay.

TABLE II Fit parameters of the integral light decay for preconditioned materials. $\tau_{90\%}$ is the time above which radiative recombination contribute over 90% to the total emission. P and NP refer to preconditioned and not preconditioned, respectively

	I_1/I_3	τ_1 (s)	I_2/I_3	τ_2 (s)	I_3	m	$\tau_{90\%}$ (s)
A-NP	2.24	2.50	0.28	6.08	1	0.90	23
A-P	2.80	2.73	0.91	5.72	1	0.99	32
B-NP	3.66	2.52	0.90	5.45	1	0.89	28
B-P	5.55	2.57	2.10	5.10	1	0.93	32
C-P	6.78	2.31	2.43	4.90	1	0.89	30

The various time constants and exponents listed in Table II do not vary greatly from one sample to another, indicating that the same mechanisms contribute in all the cases. As shown later on with the spectral analysis, the shortest lifetime, of the order of 2.5 s, seems characteristic of the phosphorescence decay following excitation by the UVs of the discharge. The second component, with lifetime of the order of 5–6 s, exhibits an emission spectrum different from the natural phosphorescence, and would correspond to chemical transformations induced by the plasma. Though these time constants are consistent with the time dependence of the spectra which was observed, the corresponding components are probably governed by more complex kinetics than a single exponential law and certainly only a rough estimation of the kinetics is obtained.

The fact that the short-lived components are somewhat enhanced after thermal treatment might be a confirmation of the photoluminescence results reported above. As a consequence, the time beyond which RIL dominated the emission is longer in preconditioned materials (cf. Fig. 7 and Table II). It is worth considering the shape of the spectra obtained in these decays.

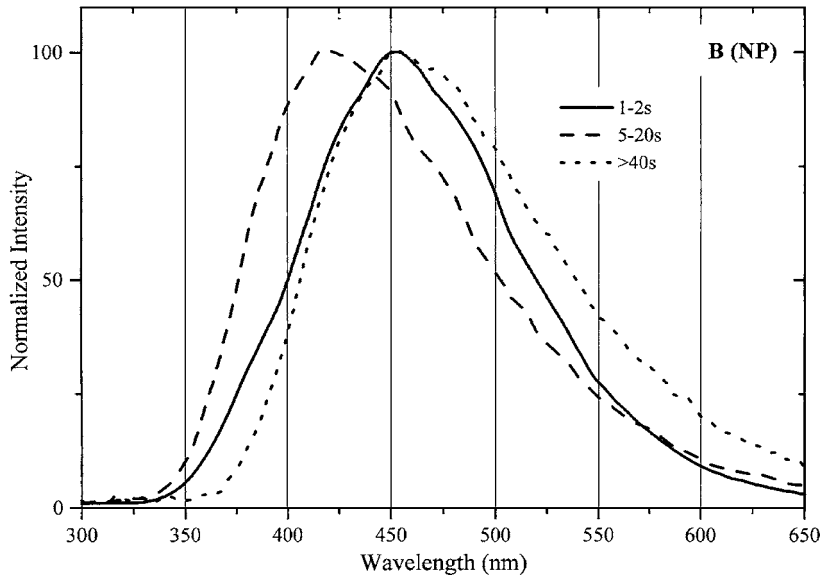

Figure 8 Time-resolved emission spectra obtained from as-received sample B after plasma interaction.

4.2.2. Time-resolved spectra

Fig. 8 shows some spectra obtained in different time intervals after plasma excitation switch off. About 15 spectra could be recorded consecutively by using integration times adapted to the signal level during the decay. The plot shows averaged spectra that are representative of the evolution. At short time, the emission peaks at about 450 nm. The shape of the spectrum is the same as that obtained in phosphorescence decay measurements. Therefore, in the time interval 1–2 s, the signal is dominated by the UV-excitation of the material.

In the time range 5–20 s, the spectrum is blue-shifted with respect to the 1–2 s range. Emission then peaks at around 415 nm. This component has been attributed to chemiluminescence due to surface transformation induced by the discharge [6]. The corresponding time constant of the order of 5–6 s may correspond either to the lifetime of the triplet state of the species formed in the excited state at the final step of a reaction, or to the kinetics of some intermediate reaction. More details on this interpretation are given elsewhere [6, 17]. At long time (>40 s), the emission peaks at about 450 nm, as in the UV-induced phosphorescence decay spectrum. The corresponding spectrum is characteristic of RIL.

Fig. 9 compares the RIL spectra obtained for the different materials that have been tested. Except for preconditioned sample A, the spectra for the different materials are approximately the same. Structures can be distinguished at about 420, 450, and 475 nm. Though these spectra are broader than those presented in Fig. 5, they exhibit the same components. It is noteworthy that the structure characteristic of sample B (Fig. 5) is apparent, and probably reinforced in the RIL spectrum (see Fig. 8).

4.2.3. Thermoluminescence

As charge recombination can be activated by thermal detrapping, some spectra were also acquired during heating of the samples. The emission spectra obtained in the temperature range [−180, −100°C] exhibit the same features as those shown in Fig. 9 for the isothermal

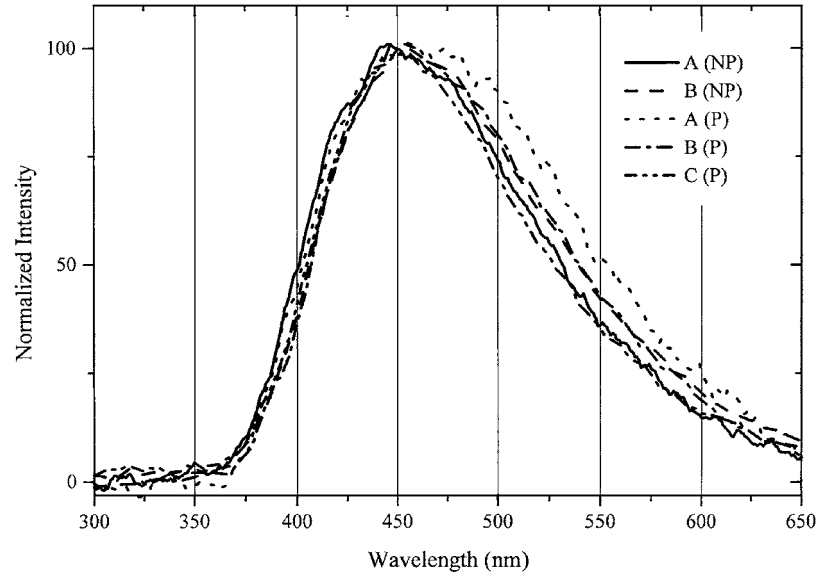

Figure 9 RIL spectra of the different materials tested.

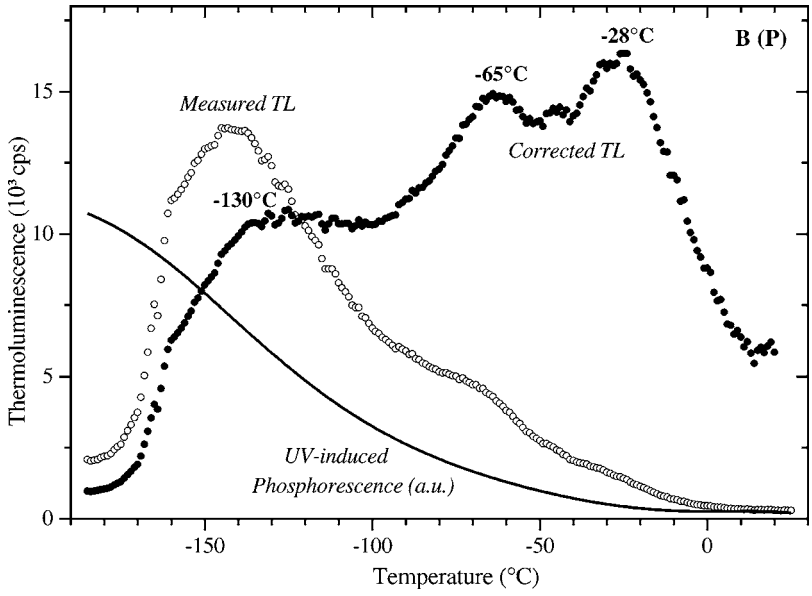

Figure 10 Thermoluminescence obtained on preconditioned sample B upon heating at 5°C/min. Correction for the temperature dependence of the UV-induced phosphorescence has been applied.

decay. This behaviour constitutes new evidence that luminescence excitation is due to charge recombination.

The activation energy of the process, the trap depth, can in principle be deduced from thermoluminescence (TL) curves, i.e. luminescence versus temperature [18]. However, the peaks observed in TL curve can also correspond to the physical disappearance of the traps, at relaxation temperatures that correspond to the onset of local molecular motions of the polymer. In that case, the deduced activation energy, even if measurable, is not necessarily related to a trap depth. A further complication is, in our opinion, the problem of the variation of the quantum efficiency of the emission as a function of temperature. Up to now, it seems not to have been considered in the literature on TL in polymers. It is probably due to the fact that wavelength-resolved spectra have been reported scarcely [19, 20], so that little was known about the origin of the emission. As we have shown that the luminescence involved in TL is phosphorescence, and that the phosphorescence itself varies strongly with temperature because of quenching effects, there is no reason to consider that the quantum efficiency of TL is not dependent on the temperature. Thus, the lower the temperature the greater the probability that a recombination event will be radiative.

Fig. 10 shows the TL curves obtained before and after correction from the temperature dependence of the main emission at about 450 nm in photoluminescence experiments. The difference in the two thermograms is considerable. The main peak occurring at low temperature becomes a shoulder after correction. For the thermally treated sample, two transition regions appear at about −120°C and −60°C. It is tempting to associate these with the γ- and β-relaxations of polyethylene which occur in the corresponding regions [21].

5. Discussion

5.1. Luminescent centres

The identification of the luminescent centres in crosslinked polyethylene is not straightforward for several reasons:

(i) the composition of the materials is very complex and there is no technique sufficiently sensitive to determine it completely.

(ii) Additives, mainly crosslinking by-products, and oxidised groups are not as well documented regarding photoluminescence as for FTIR. The documentation is limited to specific dies in liquid solution for dosimetry purpose. The response is generally dependent on the nature of the solvent, and it certainly changes is solid solution. Also, only room temperature luminescence spectra (fluorescence) are usually available. Another difficulty with luminescence techniques is that a given signature often cannot be unambiguously ascribed to a given species.

(iii) A polymeric matrix can be considered as a solid state solution wherein complex photophysical processes such as energy transfer, quenching and relaxation by non-radiative pathways are likely to occur. Only energy transfer and/or non-radiative relaxation are consistent with the fact that the emission increases after volatile species have been expelled.

In their pioneering work on the photoluminescence of low density polyethylene (LDPE), Charlesby and Partridge [20] detected a strongly structured phosphorescence peaking at around 470 nm superimposed on a broad emission with maximum at 500 nm. From comparison with model aldehyde compounds, the latter has been ascribed to oxidation groups, mainly carbonyl end groups on side chains. The main structured component of the spectrum was interpreted later on as phosphorescence from aromatic impurities [22]. Fluorescence in these additive-free materials was found at 370–380 nm. We observed phosphorescence emission at nearly 500 nm in polypropylene rather strongly oxidized [23], and so it can be inferred that the LDPE investigated in [20] was oxidized and that the strong fluorescence emission is related to this state. Though luminescence properties of LDPE and XLPE are clearly different, some common features can be envisaged in relation to residual oxidation, or to emission from aromatics,

being contaminants for LDPE and crosslinking residues for XLPE.

An optical signature resembling that of acetophenone has been detected, even in preconditioned samples for which conventional chemical analyses (FTIR and HPLC) indicated a concentration of acetophenone lower than the sensitivity limit of these techniques. Acetophenone is also detected in the decay spectra under conditions such that it should not appear, given its short phosphorescence lifetime. Its excitation might occur through energy transfer from other species. However, a peculiar feature of acetophenone is that n-π^* and π-π^* triplet levels are close lying [11, 13, 24]. As a matter of fact, the phosphorescence lifetime can change from $\approx$10 ms (n-π^* triplet state relaxation, quantum yield $\approx$0.6) to $\approx$400 ms (π-π^* triplet state relaxation, quantum yield $\approx$0.03) depending on the solvent polarity [13, 25]. A possible explanation of the current photoluminescence results is that when acetophenone is present as a free species, emission would be mostly from an n-π^* state. When acetophenone is bound, relaxation would involve π-π^* states. This interpretation is consistent with the fact that simple substituents on acetophenone lead to a π-π^* state at a lower level than n-π^*, and then emission from the former is observed [25, 26]. Other effects of the emission from π-π^* states are a more diffuse structure in the emission, and a redshift which can be of the order of 10–20 nm, depending on the nature of substituted groups or solvent polarity [25, 26]. Acetophenone would be strongly bound if grafted to the polymeric chains. However, this is normally not expected.

Another possibility is that the emission is from another species. As example, benzaldehyde exhibits an emission spectrum resembling that of acetophenone, and in a more general way, products of the form RΦ-CR′O, where Φ is an aromatic ring and R and R′ are non-polar radicals, exhibit similar phosphorescence features [27].

The above hypotheses both may explain the presence of the structure characteristic of acetophenone in the decay spectra. However, they are not consistent with the fact that the maximum emission is at around 450 nm. One can envisage that a given chromophore gives a signature that vary depending on its environment, in particular in relation to the semicrystalline nature of the material. However, groups as voluminous as acetophenone cannot fit into the crystallized regions without major distortion of the structure. Besides, it can not explain the large range of variation of the phosphorescence lifetime from one contribution to another. So, emission from other(s) specie(s) dominate these spectra. We are currently investigating the problem of reference signals by considering base resins containing selected cross-linking by-products in order to derive a fingerprint of each of them. These results will be presented in the near future. The antioxidant degradation occurring during crosslinking is a complex chemical process which leads to grafting of some cyclized groups to the polymeric chains. This constitutes another family of products which are potentially luminescent.

In fluorescence data, three regions of emission were found at 340, 360/375, and 425 nm. As preconditioning produces no clear effect on any of them, they seem related to bound species. In additive-free LDPE, fluorescence and phosphorescence have been related to the presence of unsaturated carbonyls of the enone and dienone type, respectively [28, 29]. For weakly oxidized materials, fluorescence usually peaks at about 340 nm, and phosphorescence at about 450 nm, with no structure. Fluorescence emission in the same range has been observed in the present study. However, it does not necessarily follow that the same species are involved. An emission in the range 360/375 nm has been observed for additive-free polyolefins, specially after significant thermal oxidation [30]. Results of Charlesby and Partridge also follow that trend [20]. This emission possibly reflects some oxidation of the material, consistent with the fact that it is strengthened for cable C which was stored for a long time after production.

5.2. Recombination centres

A remaining problem in the understanding of charge trapping in insulating materials is the identification of the traps. Techniques for the detection of space charge in insulators now offer high spatial resolution and sensitivity. A space charge density of 1 μC/cm^3, which is the order of magnitude being measured with modern techniques (though strongly dependent on the applied electrical stress), corresponds to a charge concentration of 6×10^{12} cm^{-3}. The concentration of repeat unit of Polyethylene (—C_2H_4—) is of the order of 6×10^{22} cm^{-3}. Hence, trapping centres concentrations down to 10^{-4} ppm are enough to explain space charge features. Such concentrations are far beyond the capabilities of conventional chemical analyses on these materials. It is also probably much lower that the actual trap concentration which can be of the order of 10^{15} cm^{-3} [31]. In this respect, RIL spectra can provide us a unique route for identifying species that are acting as recombination centres, assuming they are selectively excited in these experiments.

In our excitation conditions, the recombination-induced luminescence spectrum corresponds broadly to phosphorescence of the material. This is true even for spectra recorded during thermoluminescence. Thus, it can be inferred that recombination involves triplet states and not singlet states. From the results obtained up to now in a large variety of polyolefins, it seems this is a general rule. However, other experimental conditions may give fluorescence in spectra recorded during thermoluminescence. This is so for materials irradiated at low temperature with γ-rays [20, 31], in the absence of oxygen. In that case, the relative intensity of fluorescence increased with temperature. In presence of oxygen, fluorescence was not observed and the shape of the thermoluminescence curve considerably changed. Fluorescence was comparatively largely absent after UV-irradiation. Our conditions of excitation differ in several points from those. First, γ-irradiation produces an excitation of the bulk of the material, whereas the surface of the material only is excited during plasma contact. Second, in addition to ionization of the material surface, charges present in the discharge are also deposited on the surface. Third, molecular oxygen may

be present either in samples or in the gas used for the discharge. It is therefore expected that thermoluminescence curves and related spectra are different from those obtained after γ-irradiation.

The recombination spectra obtained for the various samples exhibit the structures found in the phosphorescence decay spectrum of preconditioned sample B, which is the most red-shifted compared to the other materials. Therefore, it seems that recombination involves preferentially the lowest lying triplet states available. These results underline the need to identify the long-lived components of the UV-induced phosphorescence.

6. Summary

The shape of the photoluminescence spectrum and emission yield of crosslinked polyethylene is strongly dependent on material processing and preconditioning. These features are related to the nature and concentration of bound and volatile luminescent centres as well as non-luminescent species that may act as quenchers. Luminescence in XLPE is difficult to interpret as there are much more chromophores that are candidates as emitting centres than in additive free polyethylenes. In the latter instance, oxidized groups are usually involved though the nature of the environment of carbonyl groups is usually poorly identified. In XLPE, emitting centres are most probably aromatic compounds but as many substituted forms coexist, since they derive from various by-products and from complex antioxidant reactions, it is quite difficult to propose an interpretation of the spectra without a previous knowledge of the signature of model compounds dispersed in a polyethylene matrix. This is why we have undertaken such an investigation on reference materials. The related results will be presented in a near future.

The identification of the phosphorescence signatures is in our opinion of great importance, because radiative charges recombination involves the lowest excited states that are available, i.e. triplet states. From such an identification, one expects to determine which species act as trapping centres in XLPE and weather the excitation of such centres may constitute a route for the electrical ageing of the material.

Acknowledgements

This work was carried out under the ARTEMIS program EU Contract Number BRPR-CT98-0724. The authors thank the ARTEMIS publications committee for permission to publish.

References

1. ARTEMIS PROGRAM, "Ageing and Reliability Testing and Monitoring of Power Cables: Diagnosis for Insulation Systems." Brite-Euram EU Contract Number BRPR-CT98-0724.
2. C. LAURENT, in Proceedings of the 6th International Conference on Conduction and Breakdown in Solid Dielectrics, Vasteras, Sweden, June 1998, IEEE N° 98CH36132, p. 1.
3. L. A. DISSADO, J. C. FOTHERGILL, A. SEE, G. C. STEVENS, L. MARKEY, C. LAURENT, G. TEYSSEDRE, U. H. NILSSON, G. PLATBROOD and G. C. MONTANARI, in Proceedings of the 2000 IEEE Conference on Electrical Insulation and Dielectric Phenomena, Victoria, Canada, Sept. 2000, IEEE N° 00CH37132, p. 136.
4. L. MARKEY, G. C. STEVENS, L. A. DISSADO and G. C. MONTANARI, in Proceedings of the 8th International Conference on Dielectric Materials, Measurements and Applications, Edinburgh, UK, Sept. 2000, IEE London N° 473, p. 413.
5. M. ALBERTINI, D. MARY and C. LAURENT, *J. Phys. D: Appl. Phys*. **30** (1997) 171.
6. F. MASSINES, P. TIEMBLO, G. TEYSSÈDRE and C. LAURENT, *J. Appl. Phys.* **81** (1997) 937.
7. P. TIEMBLO, J. M. GOMEZ-ELVIRA, G. TEYSSEDRE, F. MASSINES and C. LAURENT, *Polym. Degr. and Stability* **65** (1999) 113.
8. G. TEYSSEDRE, L. CISSE, C. LAURENT, F. MASSINES and P. TIEMBLO, *IEEE Trans. DEI* **5** (1998) 527.
9. A. C. SOMERSALL, E. DAN and J. E. GUILLET, *Macromolecules* **7** (1974) 233.
10. E. J. BOWEN, in "Luminescence in Chemistry" (van Nostrand Company, Toronto, 1968) p. 133.
11. M. KOYANAGI, R. J. ZWARICH and L. GOODMAN, *J. Chem. Phys.* **56** (1972) 3044.
12. J. T. RANDALL, *Trans. Faraday Soc.* **35** (1939) 2.
13. T. G. MATTHEWS and F. E. FYTLE, *J. Luminescence.* **21** (1979) 93.
14. Y. HAMA, Y. KIMURA, M. TSUMURA and N. OMI, *Chem. Phys.* **53** (1980) 115.
15. G. TEYSSEDRE, D. MARY and C. LAURENT, *J. Phys. D: Appl. Phys.* **31** (1998) 267.
16. R. J. FLEMING and J. HAGEKYRIAKOU, *Radiation Prot. Dosim.* **8** (1984) 99.
17. P. TIEMBLO, J. M. GOMEZ-ELVIRA, G. TEYSSÈDRE, F. MASSINES and C. LAURENT, *Polym. Degr. and Stability* **64** (1999) 67.
18. P. KIVITS and H. J. L. HAGEBEUK, *J. Luminescence* **15** (1977) 1.
19. R. J. FLEMING, *J. Thermal Analysis* **36** (1990) 331.
20. A. CHARLESBY and R. H. PARTRIDGE, *Proc. Roy. Soc. London A* **283** (1965) 312.
21. D. V. BALBACHAS and R. J. FLEMING, in Proceedings of the 1992 IEEE Conference on Electrical Insulation and Dielectric Phenomena, Victoria, Canada, Oct. 1992, IEEE N° 92CH3123-7, p. 93.
22. L. BOUSTEAD and A. CHARLESBY, *Eur. Polymer J.* **3** (1967) 459.
23. P. TIEMBLO, J. M. GOMEZ-ELVIRA, G. TEYSSEDRE and C. LAURENT, *Polym. Degr. and Stability* **68** (2000) 353.
24. G. B. STRAMBINI and W. C. GALLEY, *Chem. Phys. Lett.* **39** (1976) 257.
25. A. A. LAMOLA, *J. Chem. Phys.* **47** (1967) 4810.
26. N. C. YANG, D. S. MCCLURE, S. L. MUROV, J. J. HOUSER and R. DUSENBERY, *J. Am. Chem. Soc.* **89** (1967) 5466.
27. Z. P. LIN and W. A. AUE, *Spectrochimica Acta A* **56** (1999) 111.
28. N. S. ALLEN, J. HOMER and J. F. MCKELLAR, *J. Appl. Polym. Sci.* **21** (1977) 2261.
29. P. P. L. JACQUES and R. C. POLLER, *Eur. Polym. J.* **29** (1993) 83.
30. C. LAURENT, F. MASSINES, C. MAYOUX, D. M. RYDER and C. OLLIFF, in Proceedings of the 1995 IEEE Conference on Electrical Insulation and Dielectric Phenomena, Virginia Beach, USA, Oct. 1995, IEEE N° 95CH35842, p. 93.
31. A. CHARLESBY and R. H. PARTRIDGE, *Proc. Roy. Soc. London A* **283** (1965) 329.

Received 14 March
and accepted 4 December 2001